Mechanism of Hierarchical Porosity Development in MFI Zeolites by Desilication: The Role of Aluminium as a Pore-Directing Agent

Johan C. Groen,*[a] Louk A. A. Peffer,[a] Jacob A. Moulijn,[a] and Javier Pérez-Ramírez*[b]

Abstract: The role of the concentration and the nature of aluminium in the creation of hierarchical porosity in both commercial and synthesized MFI zeolites have been investigated through controlled mesoporosity development by desilication in alkaline medium. Framework aluminium controls the process of framework silicon extraction and makes desilication selective towards intracrystalline mesopore formation. An optimal molar Si/Al ratio in the range 25–50 has been identified; this leads to an optimal mesoporosity centred around 10 nm and mesopore surface areas of up to 235 $m^2 g^{-1}$ while preserving the intrinsic crystalline and acidic properties. At lower framework Si/Al ratios the relatively high Al content inhibits Si extraction and hardly any mesopores are created, while in highly siliceous ZSM-5 unselective extraction of framework Si induces formation of large pores. The existence of framework Al sites in different T positions that are more or less susceptible to the alkaline treatment, and the occurrence of re-alumination, are tentative explanations for the remarkable behaviour of Al in the desilication process. The presence of substantial extra framework Al, obtained by steam treatment, inhibits Si extraction and related mesopore formation; this is attributed to re-alumination of the extra-framework Al species during the alkaline treatment. Removal of extraframework Al species by mild oxalic acid treatment restores susceptibility to desilication, which is accompanied by formation of larger mesopores due to the enhanced Si/Al ratio in the acid-treated zeolite.

Keywords: aluminosilicates · aluminium · desilication · mesoporosity · zeolites

Introduction

Zeolites are crystalline aluminosilicates that possess a unique combination of properties such as high surface area, high thermal stability, intrinsic acidity, shape selectivity, and the ability to confine active metal species. As a consequence, zeolites find widespread use in industry in separation processes and as heterogeneous catalysts for oil refining and in the production of petrochemicals and fine chemicals, as well as in several environmental applications. The Brønsted acidic properties are a consequence of the presence of Al in tetrahedral coordination in the zeolite framework and enable the replacement of environmentally unfriendly mineral acids as homogeneous catalysts. The high surface area is a result of a purely microporous network of pores with molecular dimensions offering an ideal matrix for shape selectivity, but frequently at the expense of slow mass transport of reactants and products, especially when bulky molecules are involved. Zeolites could be used more efficiently if the diffusion path length of the micropores could be reduced, leading to improved transport of molecules to and from the active sites, for example by synthesis of nanocrystals[1] or by mesopore formation in larger zeolite crystals. Difficulties in the synthesis and use of nanocrystals include control of the crystal size and separation of the crystals from the reaction mixture by conventional filtration. Creation of mesoporosity in zeolite crystals has proven to be an effective approach to minimize diffusion limitations.[2,3] An attractive method of inducing mesopores is by incorporation of carbon during synthesis of the zeolite (carbon templating). To this end, porous carbon, carbon nanotubes or carbon fibres are included in the synthesis gel during hydrothermal synthesis; thus pores are left in the zeolite matrix after high-temperature combustion of the carbon–zeolite composite.[4–6] Although substantial and tunable mesoporosity can be obtained in this way by varying the amount and nature of the

[a] J. C. Groen, L. A. A. Peffer, Prof. J. A. Moulijn
DelftChemTech, Delft University of Technology
Julianalaan 136, 2628 BL Delft (The Netherlands)
Fax: (+31) 15-278-4452
E-mail: J.C.Groen@tnw.tudelft.nl

[b] Dr. J. Pérez-Ramírez
Catalan Institution for Research and Advanced Studies (ICREA)
and Institute of Chemical Research of Catalonia (ICIQ)
Av. Països Catalans s/n
43007 Tarragona (Spain)
E-mail: jperez@iciq.es

 DOI: 10.1002/chem.200500045

carbon, the crystallinity of the final product can be a problem. Moreover, this method cannot be applied easily to zeolite production on a large scale. Creation of mesoporosity by post-synthesis modification of the parent zeolite is an alternative, well-established methodology, of which one of the benefits is that it can be applied to synthesized zeolites, for example commercial samples, and thus it does not require major alteration of the synthesis procedure. De-alumination is well known in this respect;[7] it is generally achieved by steam treatment at relatively high temperatures (typically 773–873 K) or, to a greater extent, by acid leaching with, for example, nitric or hydrochloric acid solution, and leads to selective removal of Al from the framework, thereby affecting its Si/Al ratio (Scheme 1). Dislodgement of framework Al unavoidably alters the ion-exchange and acidic properties of the de-aluminated zeolite, as these are determined by the framework Al and its counterbalancing cation (typically H^+). In the case of steam treatment, extraframework aluminium species are often obtained, leading to formation of Lewis acid sites which can benefit certain catalytic applications.[8–10] Mesoporosity development by de-alumination is primarily effective for zeolites with a relatively high concentration of framework Al (a low Si/Al ratio), such as zeolite Y[11] and mordenite.[12]

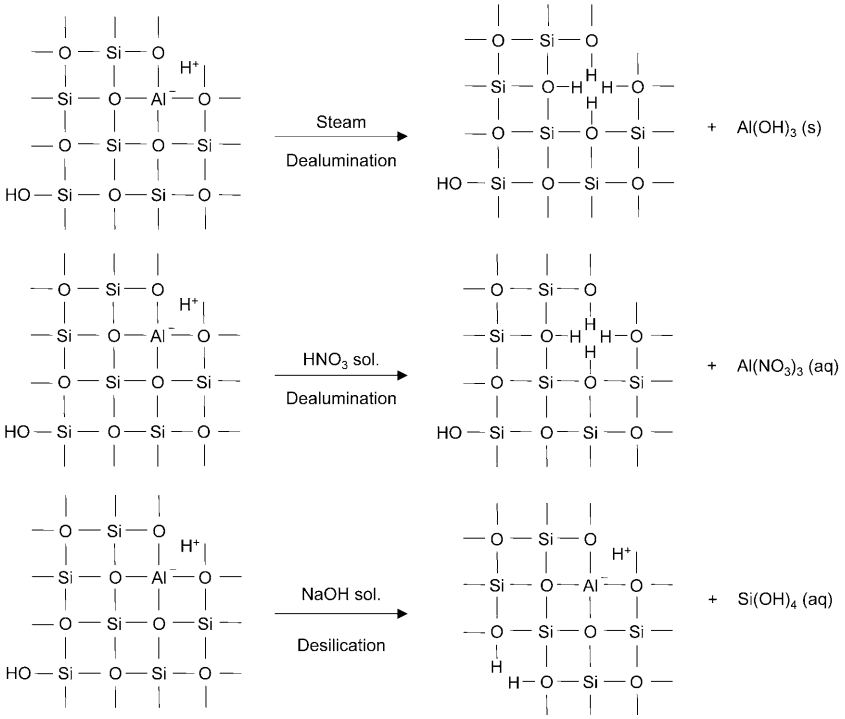

Scheme 1. Post-synthesis treatments to create mesoporosity: de-alumination upon steaming or acid treatment and desilication upon treatment in an alkaline medium.

Recently, Si extraction by treatment in aqueous alkaline solution, "desilication", has proven to be a promising method of creating mesoporosity to a greater extent than de-alumination in various zeolite structures, among which MFI zeolites appear to be very suitable.[13–19] The porosity developed seems to be obtained by preferential extraction of framework Si due to hydrolysis in the presence of OH^- ions (Scheme 1). As these observations are rather recent, a detailed mechanistic understanding of the treatment has not yet been obtained. Besides, only a few studies have been reported on the optimization of this treatment. Previous investigations have shown the influence of time and temperature of the alkaline treatment on the desilication for tuning the formation of mesoporosity.[14,17] We have recently highlighted the influence of framework aluminium on mesoporosity development in commercial zeolites by desilication.[20]

In this contribution, we elaborate on the role of Al as a pore-directing agent in the desilication of MFI zeolites upon treatment in alkaline medium. The impact of the concentration and the nature of Al on leaching of framework Si and the related development of mesoporosity has been investigated. Both commercial and synthesized MFI zeolites in a broad range of Si/Al ratios were subjected to the alkaline treatment and characterized by techniques such as N_2 adsorption, SEM, HRTEM (high-resolution electron transmission microscopy), temperature-programmed NH_3 desorption (NH_3-TPD), and Fourier transform IR (FTIR). Combination of the alkaline treatment with other post-treatments such as steaming and acid leaching enables detailed elucidation of the pore formation mechanism.

Results and Discussion

Alkaline treatment of commercial MFI zeolites

Effect of the framework Si/Al ratio on mesopore formation: N_2 adsorption measurements on the untreated commercial ZSM-5 samples lead to the characteristic isotherms resembling type I behaviour as classified by IUPAC recommendations (Figure 1).[26] Microporosity prevails in all the isotherms, as can be derived from the high uptake of N_2 at low relative pressures (<0.1). Only a small contribution of mesoporosity is observed at higher relative pressures. The *t*-plot method[24] confirms that most of the surface area ($>90\,\%$) is a result of microporosity (Table 1). Variation in the mesopore surface area (10–45 $m^2 g^{-1}$) among the various untreated zeolites is a consequence of differences in size, degree of aggregation and surface roughness of the crystals, as the

commercial zeolites mostly consist of aggregated small crystals leading to particles in the sub-micrometre range, with some intercrystalline porosity.

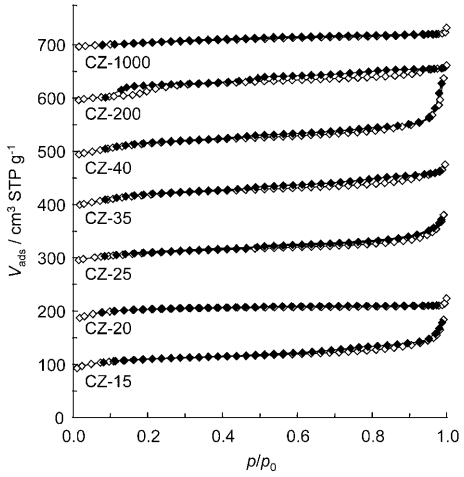

Figure 1. N_2 adsorption (◇) and desorption (◆) isotherms at 77 K of the untreated commercial MFI zeolites. For comparative purposes, the isotherms are shifted upwards with 100 $cm^3 g^{-1}$ intervals between them.

at higher relative pressures (Figure 2). The largely parallel disposition of the adsorption and desorption branches of the hysteresis loop suggests the presence of open (cylindrical) mesopores connected to the outer surface, in contrast to cavities, which give rise to a distinct broadening of the hysteresis loop by their delayed emptying along the desorption branch.[27] The latter type of pores is less suitable if the aim is to improve molecular transport by shortening of the diffusion lengths in the micropores. The mesoporosity in CZ-35-at (see Experimental Section for notation), as derived from the isotherm by application of the *t* plot, amounts to a spectacular 235 $m^2 g^{-1}$, compared with 40 $m^2 g^{-1}$ in the untreated sample. Simultaneously, the micropore volume in this particular sample decreases only about 25% and, more importantly, the size of the micropores in the alkaline-treated zeolites remains unchanged,[17] which is crucial when shape selectivity properties are desired. Ogura et al.[14] subjected CZ-20 samples to alkaline treatment by applying similar conditions; surprisingly, they reported that the isotherm of CZ-20-at hardly differed from that of the untreated zeolite, and accordingly the newly created mesoporosity was rather low. We suggested earlier that this difference in mesopore formation stems from the difference in the Si/Al ratio in the samples.[20] To support this statement, the commercial samples in Table 1, covering a broad range of Si/Al ratios, were alkaline-treated in 0.2 M NaOH at 338 K. This leads to remarkable differences in the susceptibility of the zeolites to the desilication treatment and related mesoporosity development. Representative examples are given in Figure 2, highlighting the impact of the alkaline treatment on zeolites with measured molar Si/Al ratios of 17, 37 and 176 (nominally 15, 35 and 200, respectively). At a low Si/Al ratio (CZ-15) the shape of the isotherm is hardly

Table 1. Chemical composition and textural properties of the untreated commercial MFI zeolites.

Sample[a]	Commercial code and supplier	Si/Al[b,c]	S_{BET}[d] [$m^2 g^{-1}$]	S_{meso}[e] [$m^2 g^{-1}$]	V_{micro}[e] [$cm^3 g^{-1}$]	V_{meso}[f] [$cm^3 g^{-1}$]
CZ-15-nt	CBV 3024E, Zeolyst	17	415	40	0.15	0.10
CZ-20-nt	NTZS-4, TOSOH	19	400	10	0.16	0.03
CZ-25-nt	PZ 2/40, Chemie Uetikon	26	410	35	0.16	0.10
CZ-35-nt	CBV 8020, Zeolyst	37	430	40	0.17	0.09
CZ-40-nt	CBV 8014, Zeolyst	42	415	45	0.16	0.14
CZ-200-nt	PZ 2/400, Chemie Uetikon	176	405	30	0.17	0.06
CZ-1000-nt	T-960502, TOSOH	1038	390	15	0.16	0.03

[a] The number in the sample name denotes the nominal molar Si/Al ratio. [b] Measured by ICP-OES. [c] Negligible concentration of extraframework Al species evidenced by ^{27}Al MAS-NMR. [d] BET method. [e] *t*-plot method. [f] $V_{meso} = V_{ads,p/p_0=0.99} - V_{micro}$.

Alkaline treatment of the commercial zeolites in NaOH leads to mesoporosity development, which varies dramatically for the different zeolites. Desilication of CZ-35 in alkaline medium has been shown previously to result in extraordinary changes in the adsorption properties upon treatment in 0.2 M NaOH at 338 K for 30 min.[17] The N_2 isotherm is transformed from type I to combined types I and IV, with a pronounced hysteresis loop

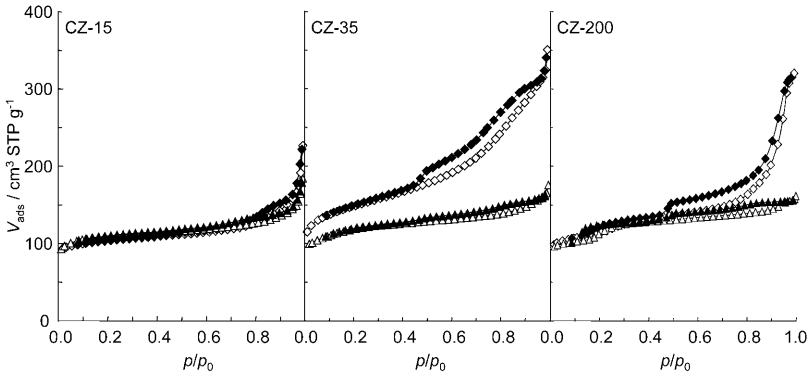

Figure 2. N_2 adsorption (open symbols) and desorption (full symbols) isotherms at 77 K of untreated (△, ▲) and alkaline-treated (◇, ◆) commercial MFI zeolites with nominal molar Si/Al ratios of 15, 35 and 200. Conditions of alkaline treatment: 0.2 M NaOH for 30 min at 338 K.

affected by the alkaline treatment, while at a high Si/Al ratio (CZ-200) the N_2 isotherm shows adsorption preferentially at relative pressures above 0.8, which indicates formation of a significant number of large pores. The alkaline-treated sample with an intermediate Si/Al ratio (CZ-35) shows particularly enhanced adsorption in the 0.4–0.8 pressure range, related to the presence of smaller mesopores in CZ-35-at than in CZ-200-at. The differences in mesoporosity development are confirmed by the Barret–Joyner–Halenda (BJH) pore size distribution (PSD) derived from the adsorption branch of the isotherm (Figure 3a). The PSDs of the untreated zeolites are plotted for comparison. Indeed, hardly any mesopore formation is evident in zeolites with a relatively low Si/Al ratio (<20) compared with untreated zeolites, as could be expected from the similar isotherms of the untreated and alkaline-treated samples. With increasing Si/Al ratios the materials become more susceptible to desilication and a mesopore size distribution centred around 10 nm is developed upon alkaline treatment (CZ35-at and CZ-40-at). The mesopore size is in good agreement with HRTEM results on the CZ-35-at sample in Figure 4, which also confirms the preservation of the microporous lattice. A further increase in the Si/Al ratio (CZ-200-at) causes a shift towards larger meso- and macropores. The PSD of CZ-200 might also suggest a well-defined distribution of pores around 2 nm. However, this contribution does not represent real pores and is caused by a fluid–crystalline-like phase transition of the adsorbed phase,[28] which is typical for ZSM-5 zeolites and depends on the framework Si/Al ratio and synthesis procedure.[29,30] The contribution should become less pronounced at lower Si/Al ratios: this correlates with the lower intensity of this peak in the alkaline-treated sample, which indeed represents a lower Si/Al ratio than the untreated zeolite because of preferential Si extraction. In CZ-1000-at, a more random distribution of mesopores, and particularly macropores, is obtained as a result of the unselective hydrolysis of T atoms from the mainly siliceous framework. Treatment of the commercial zeolites at a higher temperature (358 K) gives rise to two features of the mesoporosity formed that differ from those obtained by treatment at 338 K: 1) the PSD broadens and is shifted towards larger pore sizes; 2) the zeolites with a lower Si/Al ratio tend to become more susceptible to mesopore formation (compare Figures 3a and b). This indicates accelerated dissolution of framework Si (and Al) atoms with temperature, thereby creating larger "holes" in the zeolite crystals. Apparently the higher temperature enables the extraction of a fraction of Si atoms that would be stabilized by the neighbouring Al atoms at lower temperatures.

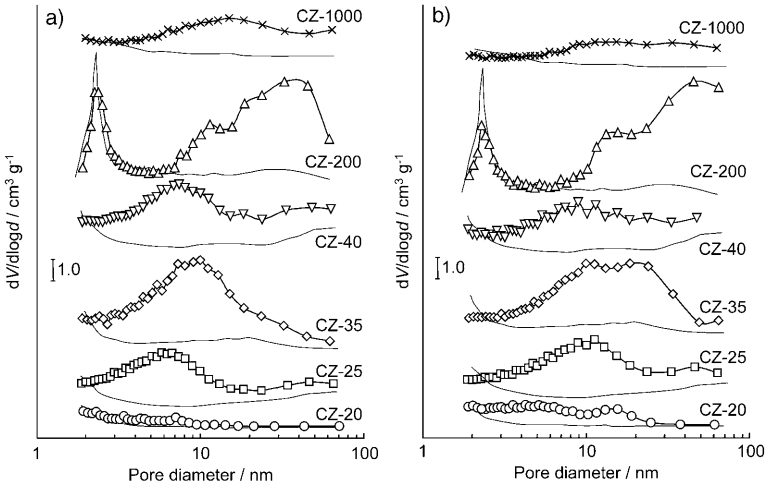

Figure 3. BJH adsorption pore size distribution of the alkaline-treated (symbols) commercial MFI zeolites upon alkaline treatment at a) 338 K and b) 358 K in 0.2 M NaOH for 30 min. The pore size distribution of the untreated samples (lines) is included for comparative purposes.

The increased surface area and volume of the mesopores upon alkaline treatment is accompanied by reduction of the micropore volume (Table 2). This decrease in micropore volume appears to be related to the degree of mesopore formation; limited mesoporosity development leads to a minor decrease in micropore volume, while at high mesopore surface areas the decrease in V_{micro} amounts to about 25%. Interestingly, the mesopore surface area and the framework Si/Al ratio are related by a volcano-type dependency (Figure 5a). ΔS_{meso} represents the increase in mesopore area as a consequence of the alkaline treatment: that is, corrected for the mesopore surface area of the untreated zeolites in Table 1. The Si/Al range of 25–50 appears to be optimal for mesopore formation, leading to increased mesopore surface areas of up to $\sim 200\ m^2 g^{-1}$ and a distribution of mesopores centred around 10 nm. The relatively low increase in mesopore surface area at Si/Al ratios <20 is a result of limited mesopore formation, as can be derived from the PSDs in Figure 3. The evolution in mesopore

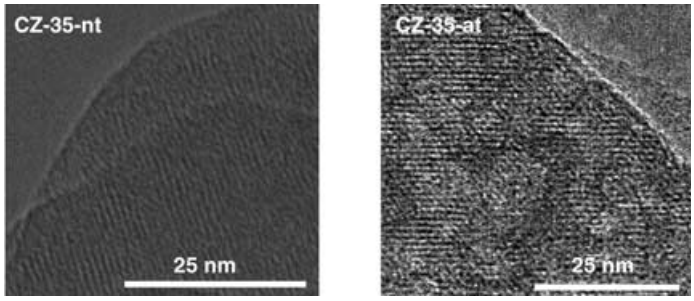

Figure 4. HRTEM micrographs of untreated and alkaline-treated CZ-35.

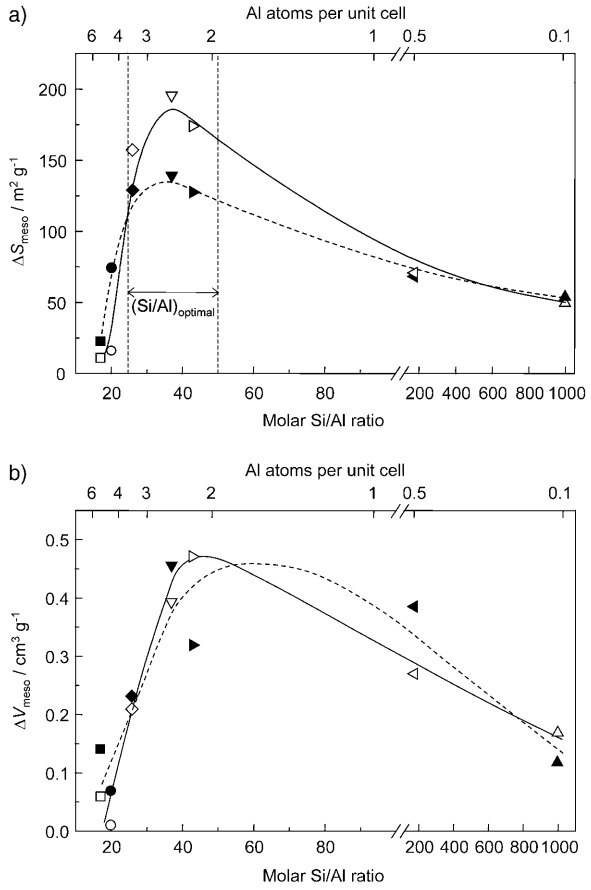

Figure 5. Variation of a) the mesopore surface area and b) the mesopore volume with the molar Si/Al ratio of the commercial MFI zeolites upon alkaline treatment in 0.2 M NaOH for 30 min at 338 K (open symbols) and 358 K (solid symbols). The secondary (upper) *x*-axis displays the equivalent number of Al atoms per unit cell associated with a certain Si/Al ratio.

surface area of the more siliceous zeolites with Si/Al ratios above 200 can be attributed to the formation of larger mesopores and macropores that should contribute mainly to the pore volume and less to the mesopore surface area. Surprisingly, the increase in mesopore volume (ΔV_{meso}) also exhibits an optimum at intermediate Si/Al ratios (Figure 5b). The limited ΔV_{meso} at low Si/Al ratios clearly results from the absence of substantial new mesoporosity in the treated materials, but the small increase in pore volume at high Si/Al ratios is at first unexpected. This observed limited change in pore volume can be explained by the formation of macropores, which are outside the conventional measuring range of N_2 adsorption at 77 K. Although the total pore volume of pores smaller than 100 nm can be measured appropriately, the contribution of larger pores to the total pore volume cannot be taken fully into account, since capillary condensation will not occur in these large pores.

Si and Al extraction upon alkaline treatment: Elemental analysis of the dried zeolites before and after the alkaline treatment, as well as analysis of the resulting filtrate, further proves the differences in susceptibility to Si and Al extraction of the zeolites with varying Si/Al ratios. At Si/Al <20 and 338 K, a relatively low Si concentration was measured in the filtrate (Figure 6), which correlates with the minor

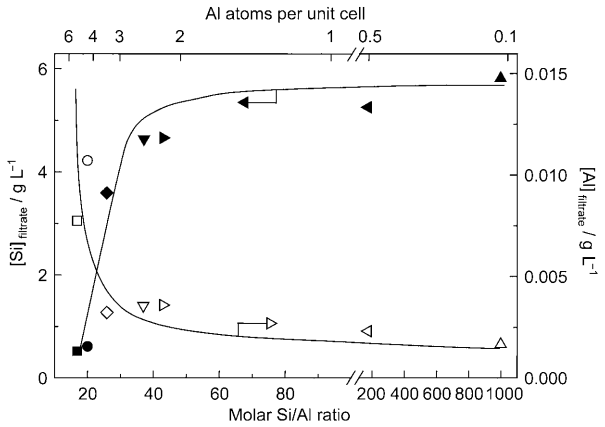

Figure 6. Concentration of Si (solid symbols) and Al (open symbols) in the filtrate obtained upon alkaline treatment of the commercial zeolites in 0.2 M NaOH for 30 min at 338 K.

degree of mesopore formation in these zeolites. The degree of Si dissolution increases with increasing Si/Al ratio, particularly in the 25–50 range. The maximum concentration of Si (approximately 6 g L^{-1}) measured in the filtrate is related to the initial concentration of OH^- ions in the alkaline solution and corresponds to about 40 wt. % Si extraction. This proves

Table 2. Chemical composition and textural properties of the alkaline-treated commercial MFI zeolites in 0.2 M NaOH for 30 min at different temperatures.

Sample	T = 338 K					T = 358 K				
	Si/Al[a]	S_{BET}[b] [m^2 g^{-1}]	S_{meso}[c] [m^2 g^{-1}]	V_{micro}[c] [cm^3 g^{-1}]	V_{meso}[d] [cm^3 g^{-1}]	Si/Al[a]	S_{BET}[b] [m^2 g^{-1}]	S_{meso}[c] [m^2 g^{-1}]	V_{micro}[c] [cm^3 g^{-1}]	V_{meso}[d] [cm^3 g^{-1}]
CZ-15-at	15	390	50	0.14	0.16	14	410	65	0.14	0.24
CZ-20-at	18	385	25	0.14	0.04	16	425	80	0.14	0.10
CZ-25-at	18	505	195	0.13	0.31	17	470	165	0.14	0.33
CZ-35-at	24	510	235	0.13	0.48	23	505	180	0.13	0.55
CZ-40-at	29	540	225	0.13	0.61	28	490	180	0.13	0.45
CZ-200-at	133	425	105	0.16	0.33	111	445	100	0.16	0.46
CZ-1000-at	560	475	75	0.16	0.20	460	440	80	0.15	0.15

[a] Measured by ICP-OES. [b] BET method. [c] *t*-plot method. [d] $V_{ads,p/p_0=0.99} - V_{micro}$.

that nearly all the OH^- is consumed for the hydrolysis of Si. Clearly, dissolution of Si is favoured over that of Al. The concentration of Al in the filtrate is more than two orders of magnitude lower than the concentration of Si (Figure 6). This can also be represented by the Si/Al ratio in the filtrate, which is generally much higher than that of the zeolites (Figure 7). In the optimal Si/Al range (25–50), the Si/Al ratio in the filtrate after treatment at 338 K amounts to ~ 1500. For zeolites with a lower Si/Al ratio this difference is not so spectacular because of the limited extraction of Si. As a consequence, the molar Si/Al ratio in the alkaline-treated zeolites decreases overall (Table 2). Furthermore, a good correlation has been established between the concentrations of Si and Al measured in the filtrates and the weight loss of the zeolites upon alkaline treatment, filtration and drying. A higher treatment temperature (358 K) in particular affects the materials with a lower Si/Al ratio and leads to enhanced Si extraction (Figure 7). Despite the considerable extraction of framework Si, the crystallinity of the alkaline-treated zeolites is mostly preserved.[17]

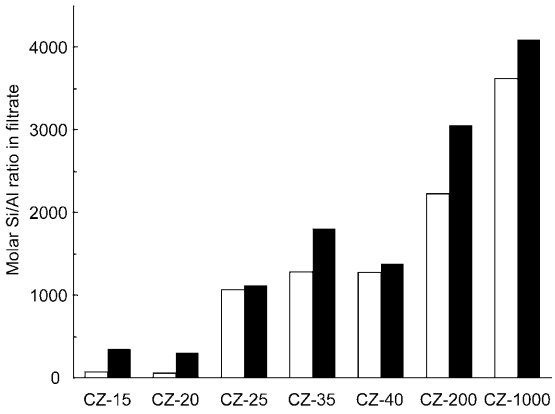

Figure 7. Molar Si/Al ratios in the filtrate obtained upon alkaline treatment of the various zeolites in 0.2 M NaOH for 30 min at 338 and 358 K; □: 338 K, ■: 358 K.

Impact of alkaline treatment on acidic properties: In contrast to de-alumination, preferential extraction of Si by treatment in alkaline medium should not substantially alter the acidic properties related to the presence of framework Al, although the substantial mesoporosity development could modify the Al environment. FTIR measurements on CZ-35 in the OH stretching region (Figure 8) confirm that a controlled alkaline treatment in general preserves the zeolite acidity, supporting previously reported NH_3-TPD results

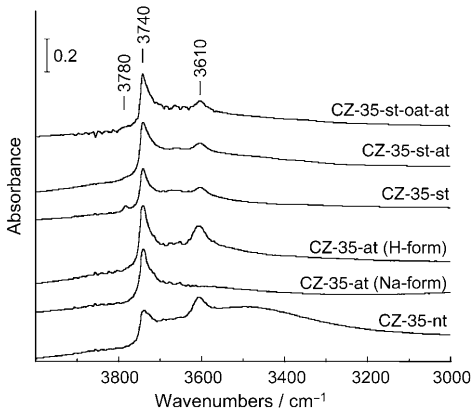

Figure 8. FTIR spectra in the OH stretching region of CZ-35 upon various treatments (see Table 3). Spectra were recorded in He at 473 K.

(see also Figure 9).[18] The absorption band at 3610 cm^{-1}, which is characteristic of Brønsted acid sites,[31] completely vanishes after alkaline treatment because of the rapid ion exchange with Na^+ cations, but is fully recovered upon ion exchange in 0.1 M NH_4NO_3 and subsequent calcination of the alkaline-treated zeolite. This preservation of acidity is applicable to the various desilicated zeolites. Interestingly,

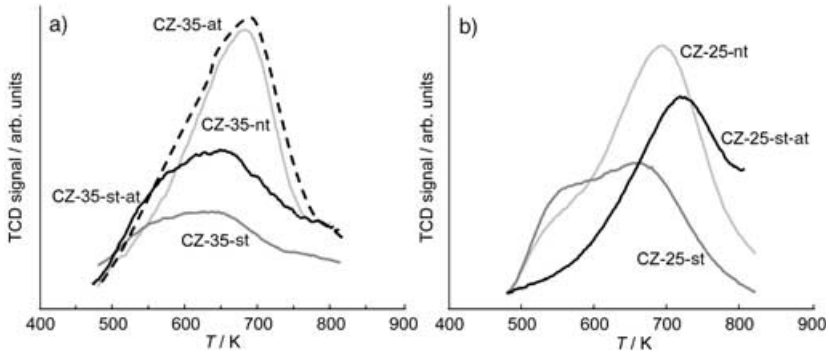

Figure 9. NH_3-TPD profiles of a) CZ-35 and b) CZ-25 upon various treatments (see Table 3).

no distinct signs of additional extra framework Al species (3660 cm^{-1})[32] can be observed in the alkaline-treated sample; this has been confirmed by ^{27}Al MAS-NMR (not shown). In CZ-35-at, the band at 3740 cm^{-1} becomes more intense while the broad band at 3590 cm^{-1} vanishes, indicating the development of isolated silanol groups and the removal of hydroxyl nests, respectively.[33] These observations do not fully corroborate the original hypothesis that mesoporosity formation is initiated preferentially at boundaries or defect sites of the zeolite crystals,[34] which would lead to a decrease in the respective absorption bands. However, the mesoporosity development is accompanied by the creation of new, isolated silanol groups at the higher "external" surface of these mesopores, inducing a more intense contribution at 3740 cm^{-1}. Moreover, if re-alumination during the treatment did occur, this would lead to "healing" of the hy-

droxyl nests, as was previously observed when zeolite beta was treated with Al isopropoxide[35] or Na aluminate,[36] and de-aluminated ultra-stable Y-sieve (USY) zeolite in alkaline medium,[37,38] and results in a further decrease in the corresponding absorption band at 3590 cm^{-1}. The possibility of re-alumination is further discussed below.

Mesopore formation mechanism: The remarkable mesoporosity development and Si extraction discussed above is determined mainly by the Si/Al ratio of the zeolites. The presence of tetrahedrally coordinated aluminium regulates the process of Si extraction and mechanism of mesopore formation according to Figure 10. As a result of the negatively

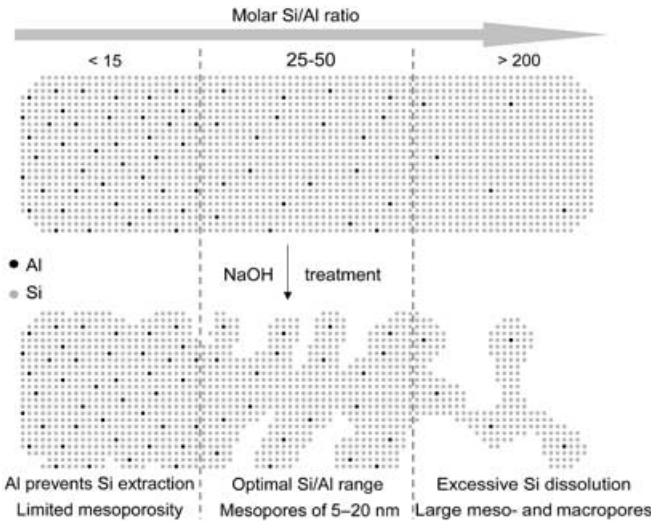

Figure 10. The influence of the Si/Al ratio on the desilication treatment of MFI zeolites in NaOH solution and the associated mechanism of pore formation.

charged AlO_4^- tetrahedra, hydrolysis of the Si–O–Al bond in the presence of OH^- is hindered compared with the relatively easy cleavage of the Si–O–Si bond in the absence of neighbouring Al.[34,39] Materials with a relatively high density of framework Al sites (low Si/Al ratio) are relatively inert to Si extraction, as most of the Si atoms are stabilized by nearby AlO_4^- tetrahedra. Consequently, these materials show a relatively low degree of Si dissolution and limited mesopore formation. Contrarily, the high density of Si atoms in zeolites with a high Si/Al ratio (low Al content) leads to substantial Si extraction and porosity development. Formation of these large pores due to the excessive Si removal is undesirable, since pores in the lower nanometre size range will already provide adequate transport characteristics to and from the active sites accompanied by only moderate Si dissolution compared with the excessive dissolution in the case of higher Si/Al ratios. An intermediate framework Al content, equivalent to a molar Si/Al ratio in the range 25–50, is optimal and leads to a relatively high degree of selective Si dissolution from which well-controlled mesopores originate.

Formation of mesopores in the nanometre size range (Figure 3) with a substantial mesopore volume (Table 2) requires the dissolution of a significant volume of the zeolite framework and consequently should be accompanied by the removal of both framework Si *and* framework Al. However, only a small fraction of the expected Al is measured in the filtrate after alkaline treatment (Figures 6 and 7). This suggests that not all the Al removed from the framework during the alkaline treatment remains in the liquid phase, but is somehow re-incorporated in the solid. Particularly when the pH decreases due to consumption of OH^- ions during the alkaline treatment, the solubility of Al decreases and deposition is promoted.[40,41] For zeolites with a molar Si/Al ratio in the range 25–50, a decrease is typically observed from pH 13.3 to 12.2, which indicates that more than 90% of the initial OH^- ions have been consumed. Deposition of Al species during the alkaline treatment is further supported by the observations[14,17] that the Al concentration in the filtrate decreases when the duration of the alkaline treatment is increased, while the Si concentration increases progressively. Formation of amorphous extra framework aluminium oxide or aluminosilicate could occur, but this would typically lead to extra bands in the FTIR spectra around 3660 cm^{-1}, which were not observed in our spectra. The Brønsted acidity seems to be preserved (FTIR and NH_3-TPD),[17,18] and even increases due to the lower Si/Al ratio of the resulting alkaline-treated sample; this suggests that most of the Al atoms in the alkaline-treated sample are in framework positions and indicates that part of the Al extracted during the alkaline treatment has been re-inserted in the zeolite framework (re-alumination), as has already been noticed on the basis of FTIR[42,43] and ^{27}Al MAS-NMR measurements.[43,44] The re-aluminated Al species should preferably be located close to the mesopores since this is where most of the vacancies are created during the desilication process. Consequently, in principle these newly created Al sites should have excellent accessibility.

The coexistence of various Al sites which are more or less susceptible to hydrolysis in NaOH solution is strongly suggested by the observations that 1) mesopores are created which size clearly depends on the framework Al concentration and 2) the filtrate contains a much smaller fraction of the expected Al. The existence of different framework Al sites with a different tendency to be extracted has been previously reported for zeolite beta, in which de-alumination and re-alumination seem to occur for specific T1 and T2 sites in the framework.[35] Similar conclusions on the re-alumination of specific T sites during treatment of zeolite beta with a $NaAlO_2$ solution were derived by Zaiku et al.[36] ^{27}Al MQ-MAS NMR measurements by Sarv et al.[45] have also confirmed the existence of different Al sites in zeolite ZSM-5, which supports our hypothesis on the role of Al during the desilication process. Forthcoming MQ-MAS NMR investigations should confirm changes in the ratio of Al in different T positions before and after alkaline treatment.

Nonframework aluminium as pore-directing agent? Not only the concentration, but also the nature of the aluminium and its location, may play a role in desilication by alkaline treatment. To investigate the impact of extraframework aluminium (Al_{EF}), some of the commercial zeolites were steam-treated at 873 K for 5 h. This induces dislodgement of lattice Al into non-lattice positions. As expected, the molar Si/Al ratio of the zeolites as determined by inductively coupled plasma optical emission spectroscopy (ICP-OES) is not affected by the steam treatment (Table 3 for CZ-35). A broad absorption band that appears at 3660 cm^{-1} in the FTIR spectrum of CZ-35-st (Figure 8) is ascribed to hydroxyl groups connected to Al_{EF} species.[32] In addition, a weak band at 3780 cm^{-1} is observed, which is assigned to hydroxyl groups connected to partially framework Al species, which are not in pure tetrahedral coordination.[46] NH_3-TPD measurements on the steamed samples also confirm distinct changes in acidity related to the extraction of Al from the framework, extensively depleting Brønsted acid sites (Figure 9). The intensity of the peak around 673 K, which represents strong acidity and is associated with lattice Al, is reduced, while the low-temperature contribution (ca. 550 K) related to NH_3 desorption from weakly acid sites (probably of Lewis nature) increases. The total acidity in the steamed sample is much lower than that of the untreated sample, suggesting significant clustering of the Al_{EF} species.

Importantly, the porosity development in the steamed sample is very limited compared with the alkaline-treated zeolite. The mesopore surface area only increases from 40 $m^2 g^{-1}$ in CZ-35-nt to 55 $m^2 g^{-1}$ in CZ-35-st (Table 3), in contrast to 235 $m^2 g^{-1}$ in the alkaline-treated sample CZ-35-at. Furthermore, the resemblance of the BJH adsorption PSD of CZ-35-st to that of CZ-35-nt confirms the negligible mesoporosity development (Figure 11). Moreover, a slight decrease in micropore volume is observed, probably related to the blockage of some microporosity by Al_{EF} species. These results confirm that in the optimal Si/Al range of 25–50 desilication is superior to de-alumination as a post-treatment for mesoporosity development in MFI zeolites (Figure 12). At lower Si/Al ratios (and higher framework Al concentrations, as in CZ-15) de-alumination and desilication seem to result in similar but only minor mesoporosity development, while at high Si/Al ratios (CZ-200) desilication is still favorable because of the extremely low framework Al content that can be extracted by de-alumination.

Based on the mesopore formation mechanism proposed in the previous section, alkaline treatment of hydrothermally de-aluminated samples should result in more extensive Si dissolution and formation of preferentially larger pores, a consequence of the higher framework Si/Al ratio. However, the steamed sample appears to be less susceptible to the alkaline treatment than the untreated sample, as can be deduced from the concentration of Si and Al in the filtrate and the porosity development. Table 3 shows that the Si concentration in the filtrate upon alkaline treatment of CZ-35-st is about three times lower than that of CZ-35-at. Additionally, the Al concentration is about four times higher, which can be explained by the dissolution in the alkaline medium of Al_{EF} species that can remain in solution as a result of the lower consumption of OH^- ions, that is, at higher pH. The disappearance of the absorption band at

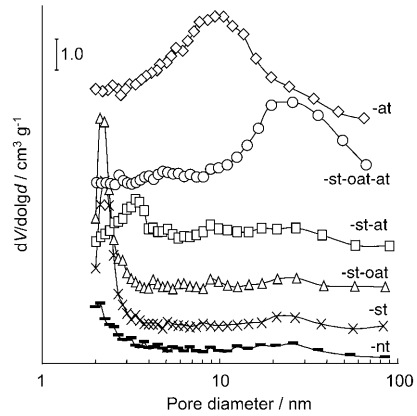

Figure 11. BJH pore size distribution of CZ-35 upon various treatments (see Table 3).

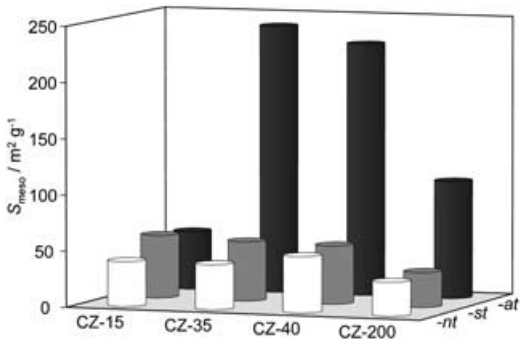

Figure 12. Evolution of the mesopore surface area of selected zeolites upon various treatments (see Table 3).

Table 3. Chemical and textural properties of CZ-35 upon different treatments and their combinations.

Sample	Treatment	Si/Al[a]	$[Si]_{filtrate}$[a] [$g L^{-1}$]	$[Al]_{filtrate}$[a] [$g L^{-1}$]	S_{BET}[b] [$m^2 g^{-1}$]	S_{meso}[c] [$m^2 g^{-1}$]	V_{micro}[c] [$cm^3 g^{-1}$]	V_{meso}[d] [$cm^3 g^{-1}$]
CZ-35-nt	untreated	37	–	–	430	40	0.17	0.09
CZ-35-at	alkaline	24	4.64	0.004	510	235	0.13	0.48
CZ-35-st	steam	39	–	–	375	55	0.16	0.11
CZ-35-st-oat	steam + oxalic acid	60	–	–	385	55	0.16	0.12
CZ-35-st-at	steam + alkaline	38	1.65	0.015	415	80	0.15	0.16
CZ-35-st-oat-at	steam + oxalic acid + alkaline	46	3.20	0.006	405	100	0.13	0.27

[a] Measured by ICP-OES. [b] BET method. [c] *t*-plot method. [d] $V_{ads,p/p_0=0.99} - V_{micro}$.

3780 cm^{-1} and a slight decrease in the absorption band at 3660 cm^{-1} are evident in the FTIR spectrum of the steamed sample after a subsequent alkaline treatment, confirming the dissolution of Al_{EF} species created by steaming. Interestingly, NH_3-TPD of CZ-35-st-at implies a partial recovery of the original acidic properties (Figure 9a). The high-temperature contribution (strong acidity) clearly intensifies upon alkaline treatment of the steamed sample, strongly suggesting a partial re-alumination of the Al_{EF} species, since the Si/Al ratio does not change significantly. This effect is even more pronounced in the CZ-25 series, while Si/Al (22) in CZ-25-st-at is only slightly lower than Si/Al (26) in the untreated and steamed samples (Figure 9b). In agreement with the ICP results, N_2 adsorption also reveals that the alkaline treatment of the steamed sample is less efficient than that of the untreated sample; this is supported by the PSD in Figure 10 and the data in Table 3. A much smaller proportion of mesopores has been formed upon alkaline treatment of the steamed sample (CZ-35-st-at) than in CZ-35-at, which is tentatively attributed to the surpressing role of Al_{EF} species.

Although Al_{EF} species could dissolve in the alkaline medium and therefore interfere with the Si extraction, the relatively low content of Al should not affect the consumption of OH^- ions significantly. To eliminate Al_{EF} species, before the alkaline treatment the steamed sample was treated in 0.1 M oxalic acid at 343 K, which preferentially removes these extra framework species while not significantly affecting framework Al.[47] Indeed, ICP analysis of the steamed zeolite before and after oxalic acid treatment shows a significant increase in the molar Si/Al ratio of CZ-35-st-oat (to Si/Al 60:1). The untreated zeolite was also treated in oxalic acid under similar conditions; as expected, neither the Si/Al ratio nor the acidic properties were affected. The analogous results from NH_3-TPD and FTIR of CZ-35-nt-oat and CZ-35-nt confirm 1) the inertness of framework Al to the oxalic acid treatment and 2) the negligible content of extra framework species in the untreated sample. Alkaline treatment of CZ-35-st-oat leads to spectacular changes compared with CZ-35-st-at (which is without an interim oxalic acid treatment). As can be deduced from Table 3 and Figure 10, the Si extraction of 3.2 $g\,L^{-1}$ measured in the filtrate and the porosity development upon alkaline treatment of the steamed sample with the additional oxalic acid treatment are much higher. The mesopore volume of 0.27 $cm^3\,g^{-1}$ in CZ-35-st-oat-at is significantly higher than that (0.16 $cm^3\,g^{-1}$) of the alkaline-treated steamed sample. Interestingly, the sample does not only show a higher degree of mesopore formation than CZ-35-st-at, but also contains larger pores than CZ-35-at. This shift in pore size is attributed to the higher framework Si/Al ratio of CZ-35-st-oat, supporting the proposed mechanism of mesopore formation in Figure 10. Despite the larger pore size in CZ-35-st-oat-at, the pore volume (0.27 $cm^3\,g^{-1}$) is lower than that in CZ-35-at (0.48 $cm^3\,g^{-1}$). The reason for this is twofold. CZ-35-st-oat-at has a somewhat lower susceptibility to Si extraction than CZ-35-at, as can be deduced from the lower Si concentration in the filtrate, which is probably a result of some Al_{EF} species remaining after the oxalic acid treatment. Besides, larger pores are created in CZ-35-st-oat-at that cannot be fully assessed by N_2 adsorption.

On the basis of the observations above, the role of the Al_{EF} species can be described tentatively as follows: Al_{EF} species, created for example by steam treatment, will dissolve at high pH (pH ~13) and are subsequently re-aluminated during the alkaline treatment at lower pH (pH ~11–12). Re-alumination of dissolved Al_{EF} will occur particularly at structural vacancies, which are available extensively at the outer surface of the crystals where Si has been extracted. This will lead to an Al-rich outer surface, and accordingly during the treatment the zeolite will become less susceptible to Si extraction, as can be deduced from Figures 5 and 10. Upon removal of the extra framework species by oxalic acid, the zeolite will act like an untreated material with a higher Si/Al ratio, it will be more susceptible to the alkaline treatment and larger mesopores will be formed. The effect of the various treatments and their combination on the development of porosity is represented in Figure 13.

Re-alumination of Al_{EF} species upon alkaline treatment has been reported previously by Lietz et al.,[42] who investigated the modification of the catalytic properties, for conversion of propane and methanol, of calcined and steamed ZSM-5 zeolite upon treatment in NaOH solution. Disappearance of the IR absorption band at 3660 cm^{-1}, which is characteristic for Al_{EF} species, was observed in the steamed zeolite after treatment in NaOH. In addition, the absorption band at 3610 cm^{-1} associated with Brønsted acid sites, that is, framework Al, was recovered. In agreement with our findings, these authors also observed decreased dissolution of Si for the steamed sample compared with the calcined zeolite.

Synthesized zeolites: In addition to the above study of commercial zeolites, zeolites with Si/Al ratios of 36 (SZ-35) and >2000 (SZ-2000) were synthesized and post-treated to confirm the universal effect of the alkaline treatment and the validity of the mesopore formation mechanism derived therefrom. Figure 14 shows that SZ-35 consists of larger particles (~3 μm) than those (<1 μm) generally observed in the commercial zeolites, and in particular in CZ-35 with a similar Si/Al ratio. As a consequence, the mesopore surface area of SZ-35-nt (15 $m^2\,g^{-1}$; Table 4) is considerably lower than the 40 $m^2\,g^{-1}$ in CZ-35-nt. The purely siliceous SZ-2000 consists of elongated hexagonal crystals, length ~60 μm, and shows an even lower mesopore surface area of ~5 $m^2\,g^{-1}$.

Importantly, the mesoporosity development in the alkaline-treated synthesized zeolites correlates perfectly with the trend in the commercial zeolites. The increase in mesopore surface area of SZ-35-at amounts to 200 $m^2\,g^{-1}$, which, based on the Si/Al ratio of 36 in the untreated material, fits well in the optimum of the volcano plot in Figure 5 and is very similar to the increase of 195 $m^2\,g^{-1}$ upon alkaline treatment of CZ-35. Contrarily, SZ-2000-at shows a negligible increase in

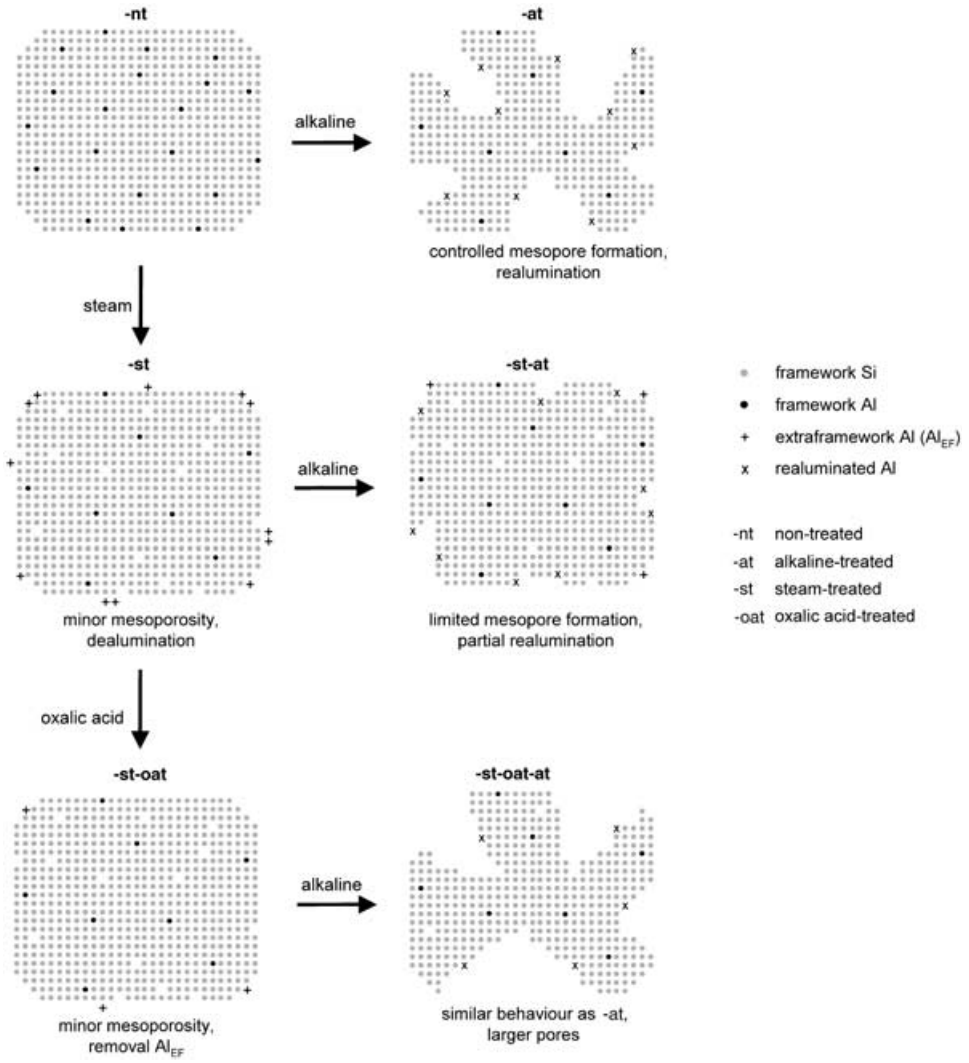

Figure 13. Schematic proposed hierarchical evolution of mesoporosity upon various treatments and their combinations.

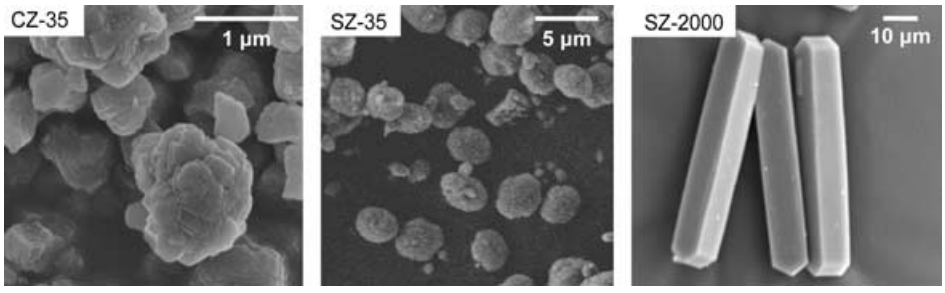

Figure 14. SEM micrographs of selected untreated zeolites.

mesopore surface area of 5 $m^2 g^{-1}$, which should be attributed to a progressive dissolution of the siliceous crystals in the absence of the pore-directing framework Al species. Moreover, the mesopore size distribution developed in SZ-35-at coincides with that of CZ-35-at (Figure 15). This proves the universal character of this treatment and further supports the suggestion that the mechanism of intracrystalline mesopore formation is primarily to the Si/Al ratio of the untreated zeolite. In particular, the intracrystalline mesopore formation will significantly improve the transport properties to and from the active sites present in the micropores, with the prospect of more efficient utilization of zeolite crystals in catalytic processes.

Conclusion

Aluminium in framework positions directs the preferential extraction of framework Si upon alkaline treatment of MFI zeolites, leading to controlled mesopore formation. An optimal molar framework Si/Al range of 25–50, has been identified, leading to increased mesopore surface areas of up to about 200 $m^2 g^{-1}$ coupled with a decrease of less than 25% in micropore volume and preservation of the micropore size. At higher Si/Al ratios uncontrolled extraction of Si occurs, leading to large pores, while a high Al content (low Si/Al ratio) leads to restricted Si extraction and minor mesoporosity development. The preservation of the acidic properties of the alkaline-treated zeolites coupled to spectacular mesopore formation implies re-alumination of extracted Al species, which should lead to easily accessible acidity. Alkaline treatment of both commercial and synthesized MFI zeolites leads to very similar results and confirms the universality of the alkaline treatment and the process of intracrystalline mesopore formation. A high concentration of extra framework Al species, as created by steam treatment, inhibits Si extraction and connected mesoporosity development; this is tentatively attributed to re-alumination of the extra framework species at the outer surface. A mild oxalic acid treatment of the steamed zeolite removes extra

Table 4. Chemical and textural properties of untreated and alkaline-treated synthesized zeolites.

Sample	Si/Al[a]	S_{BET}[b] [$m^2 g^{-1}$]	S_{meso}[c] [$m^2 g^{-1}$]	V_{micro}[c] [$cm^3 g^{-1}$]	V_{meso}[d] [$cm^3 g^{-1}$]
SZ-35-nt	36	410	15	0.17	0.03
SZ-35-at	n.m.[e]	555	215	0.14	0.34
SZ-2000-nt	>2000	360	5	0.17	0.02
SZ-2000-at	n.m.	355	10	0.17	0.04

[a] Measured by ICP-OES. [b] BET method. [c] *t*-plot method. [d] $V_{ads,p/p_0=0.99} - V_{micro}$. [e] n.m., not measured.

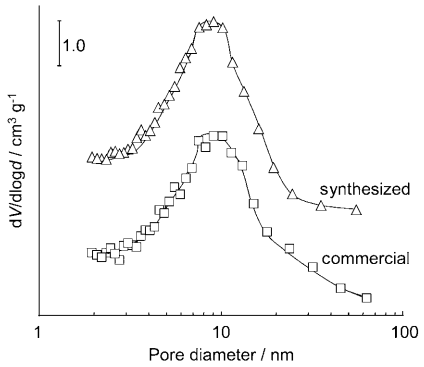

Figure 15. BJH adsorption pore size distribution of (□) CZ-35-at and (△) SZ-35-at upon treatment in 0.2 M NaOH at 338 K for 30 min.

framework Al and recovers susceptibility to desilication accompanied by formation of larger mesopores as a result of the higher framework Si/Al ratio.

Experimental Section

Materials and treatments

Parent zeolites: Various commercial and synthesized MFI zeolites, denoted as CZs and SZs respectively, were used. Table 1 shows the commercial ZSM-5 zeolites supplied by various manufacturers; they cover a broad range of nominal molar Si/Al ratios (15–1000). ZSM-5 with a molar Si/Al ratio of ~35 (SZ-35) was prepared by hydrothermal synthesis in an alkaline medium with tetrapropylammonium ions (TPA) as the template.[21] The seeding gel, prepared by adding silicic acid to the basic solution of TPAOH and NaOH, was mixed and shaken vigorously with the synthesis gel consisting of sodium aluminate, NaOH solution and silicic acid. The gel obtained in this way was then transferred to a Teflon-lined stainless steel autoclave and kept in a static air oven at 453 K for 40 h. The solid product was recovered by filtration and washed with demineralized water.

Pure silica MFI (silicalite) (SZ-2000) was synthesized using fluoride ions as a mineralizing agent.[22] Ludox HS suspension (40 wt.%) was used as the silica source and stirred to homogeneity with NaF, HF and TPABr. Incubation of the gel at 443 K for 60 h in a Teflon-lined stainless steel autoclave was followed by filtration and washing with demineralized water.

The template in the as-synthesized samples was removed by calcination in air at 823 K for 10 h using a ramp of 2 K min^{-1}. The calcined zeolite was then converted into the H-form by three consecutive exchanges with an ammonium nitrate solution (0.1 M) and subsequent calcination at 823 K for 5 h with the same temperature ramp.

Throughout this account, the suffix -nt refers to untreated samples, -st to steamed samples, -oat to oxalic acid-treated samples, and -at to alkaline-treated samples. Combinations of treatments are denoted by the appropriate suffices according to the time sequence of the treatments applied. For example, CZ-35-st-oat-at refers to the commercial zeolite with a nominal Si/Al ratio of 35 that has been successively steamed, then treated with oxalic acid and finally submitted to alkaline treatment.

Steam treatment: The zeolites underwent steam treatment in a quartz fixed-bed reactor in a flow of steam (water partial pressure = 300 mbar) and helium (30 $cm^3 min^{-1}$) at atmospheric pressure and 873 K for 5 h, after heating in He with a temperature ramp of 10 K min^{-1}.

Oxalic acid treatment: Oxalic acid treatment was applied in order to remove Al_{EF} species created by steam treatment: each sample (500 mg) was stirred in 0.1 M oxalic acid at 343 K for 2 h. The resulting product was filtered, washed carefully with demineralized water and dried overnight at 373 K.

Alkaline treatment: The zeolites were treated with an aqueous NaOH solution (0.2 M) at 338 and 358 K: each sample (330 mg) was stirred vigorously in NaOH solution (10 mL)in a polypropylene flask for 30 min at a specific temperature. The reaction was quenched by submersion of the flask in an ice–water mixture; the solid product was then filtered, washed thoroughly with demineralized water, dried overnight at 373 K.

Characterization: N_2 adsorption at 77 K was performed in a Quantachrome Autosorb-6B gas adsorption analyser to derive information on the porous characteristics of the untreated and treated samples. Before the adsorption measurement the samples were treated in vacuum at 573 K for 12 h. The BET method[23] was applied in the adapted relative pressure range of 0.01–0.1 to calculate the total surface area, while the *t*-plot method[24] was used to discriminate between micro- and mesoporosity. In the *t*-plot, the reported mesopore surface area (S_{meso}) consists of contributions from the outer surface of the particles as well as mesopores and macropores. The BJH model[25] applied to the adsorption branch of the isotherm provides information on the mesopore size distribution. Si and Al concentrations in the zeolites and in the filtrates obtained upon alkaline treatment were determined by ICP-OES in a Perkin–Elmer Optima 3000DV. The crystal size and morphology of the untreated and treated zeolites were investigated by SEM on JEOL JSM-6700F and Philips XL-20 microscopes. HRTEM investigations were performed on a Philips CM30UT electron microscope. FTIR spectra were recorded in He at 473 K on a Nicolet Magna 860 Fourier transform spectrometer using a Spectratech diffuse reflectance (DRIFT) accessory, equipped with a high-temperature cell. The sample was pretreated at 723 K in a flow of He to remove any contaminants. NH_3-TPD was carried out in a Micromeritics TPR/TPD 2900 system equipped with a thermal conductivity detector (TCD). The sample (25 mg) was pretreated at 823 K in He for 1 h. Afterwards, pure NH_3 (25 $cm^3 min^{-1}$) was adsorbed at 473 K for 10 min. Subsequently a flow of He (25 $cm^3 min^{-1}$) was passed through the reactor for 20 min to remove weakly adsorbed NH_3 from the zeolite. This procedure was repeated three times. Desorption of NH_3 was monitored in the range 473–823 K.

Acknowledgements

The authors are indebted to Dr. P. J. Kooyman (Delft University of Technology, The Netherlands) for HRTEM investigations. T. Bach (Hydro ASA, Norway) and M. de Niet (Delft University of Technology, The Netherlands) are gratefully acknowledged for SEM measurements. The assistance of O. Landman (Delft University of Technology, The Netherlands) in performing the alkaline treatments is highly appreciated.

[1] J. Aguado, D. P. Serrano, J. M. Escola, J. M. Rodríguez, *Microporous Mesoporous Mater.* **2004**, *75*, 41–49.
[2] C. H. Christensen, K. Johannsen, I. Schmidt, C. H. Christensen, *J. Am. Chem. Soc.* **2003**, *125*, 13370–13371.
[3] C. H. Christensen, I. Schmidt, C. H. Christensen, *Catal. Commun.* **2004**, *5*, 543–546.

[4] I. Schmidt, A. Boisen, E. Gustavsson, K. Ståhl, S. Pehrson, S. Dahl, A. Carlsson, C. J. H. Jacobsen, *Chem. Mater.* **2001**, *13*, 4416–4418.
[5] Y. Tao, Y. Hattori, A. Matumoto, H. Kanoh, K. Kaneko, *J. Phys. Chem. B* **2005**, *109*, 194–199.
[6] A. H. Janssen, I. Schmidt, C. J. H. Jacobsen, A. J. Koster, K. P. de Jong, *Microporous Mesoporous Mater.* **2003**, *65*, 59–75.
[7] J. Scherzer, *ACS Symp. Ser.* **1984**, *248*, 157–200.
[8] J. A. van Bokhoven, M. Tromp, D. C. Koningsberger, J. T. Miller, J. A. Z. Pieterse, J. A. Lercher, B. A. Williams, H. H. Kung, *J. Catal.* **2001**, *202*, 129–140.
[9] E. J. M. Hensen, Q. Zhu, R. A. van Santen, *J. Catal.* **2003**, *220*, 260–264.
[10] J. Pérez-Ramírez, F. Kapteijn, J. C. Groen, A. Doménech, G. Mul, J. A. Moulijn, *J. Catal.* **2003**, *214*, 33–45.
[11] A. H. Janssen, A. J. Koster, K. P. de Jong, *Angew. Chem.* **2001**, *113*, 1136–1138; *Angew. Chem. Int. Ed.* **2001**, *40*, 1102–1104.
[12] S. van Donk, A. H. Janssen, J. H. Bitter, K. P. de Jong, *Catal. Rev.* **2003**, *45*, 297–319.
[13] M. Ogura, S. Shinomiya, J. Tateno, Y. Nara, E. Kikuchi, M. Matsukata, *Chem. Lett.* **2000**, 882–883.
[14] M. Ogura, S. Shinomiya, J. Tateno, Y. Nara, M. Nomura, E. Kikuchi, M. Matsukata, *Appl. Catal. A* **2001**, *219*, 33–43.
[15] T. Suzuki, T. Okuhara, *Microporous Mesoporous Mater.* **2001**, *43*, 83–89.
[16] J. C. Groen, J. Pérez-Ramírez, L. A. A. Peffer, *Chem. Lett.* **2002**, 94–95.
[17] J. C. Groen, L. A. A. Peffer, J. A. Moulijn, J. Pérez-Ramírez, *Colloids Surf. A* **2004**, *241*, 53–58.
[18] J. C. Groen, L. A. A. Peffer, J. A. Moulijn, J. Pérez-Ramírez, *Microporous Mesoporous Mater.* **2004**, *69*, 29–34.
[19] L. Su, L. Liu, J. Zhuang, H. Wang, Y. Li, W. Shen, Y. Xu, X. Bao, *Catal. Lett.* **2003**, *91*, 155–167.
[20] J. C. Groen, J. C. Jansen, J. A. Moulijn, J. Pérez-Ramírez, *J. Phys. Chem. B* **2004**, *108*, 13062–13065.
[21] *Verified Syntheses of Materials* (Eds.: H. Robson, K. P. Lillerud), Elsevier, Amsterdam, **2001**, p. 198.
[22] C. I. Round, C. D. Williams, K. Latham, C. V. A. Duke, *Chem. Mater.* **2001**, *13*, 468–472.
[23] S. Brunauer, P. H. Emmett, E. Teller, *J. Am. Chem. Soc.* **1938**, *60*, 309–319.
[24] B. C. Lippens, J. H. de Boer, *J. Catal.* **1965**, *4*, 319–323.
[25] E. P. Barret, L. G. Joyner, P. H. Hallenda, *J. Am. Chem. Soc.* **1951**, *73*, 373–380.
[26] K. S. W. Sing, D. H. Everett, R. A. W. Haul, L. Moscou, R. A. Pierotti, J. Rouquerol, T. Siemieniewska, *Pure Appl. Chem.* **1985**, *57*, 603–619.
[27] J. C. Groen, J. Pérez-Ramírez, *Appl. Catal. A* **2004**, *268*, 121–124.
[28] P. L. Llewellyn, J. P. Coulomb, Y. Grillet, J. Patarin, H. Lauter, H. Reichert, J. Rouquerol, *Langmuir* **1993**, *9*, 1852–1856.
[29] J. C. Groen, L. A. A. Peffer, J. Pérez-Ramírez, *Microporous Mesoporous Mater.* **2003**, *43*, 1–17.
[30] A. Saito, H. C. Foley, *Microporous Mater.* **1995**, *3*, 543–556.
[31] A. Zecchina, S. Bordiga, G. Spoto, D. Scarano, G. Petrini, G. Leofanti, M. Padovan, *J. Chem. Soc. Faraday Trans.* **1992**, *88*, 2959–2969.
[32] I. Kiricsi, C. Flego, G. Pazzuconi, W. O. Parker, R. Millini, C. Perego, G. Bellussi, *J. Phys. Chem.* **1994**, *98*, 4627–4634.
[33] A. Zecchina, S. Bordiga, G. Spoto, L. Marchese, G. Petrini, G. Leofanti, M. Padovan, *J. Phys. Chem.* **1992**, *96*, 4991–4997.
[34] A. Cižmek, B. Subotić, I. Šmit, A. Tonejc, R. Aiello, F. Crea, A. Nastro, *Microporous Mater.* **1997**, *8*, 159–168.
[35] A. Omegna, J. A. van Bokhoven, G. Pirngruber, R. Prins, *Phys. Chem. Chem. Phys.* **2004**, *6*, 447–452.
[36] X. Zaiku, B. Jianqing, Y. Yiqing, C. Qingling, Z. Chengfang, *J. Catal.* **2002**, *205*, 58–66.
[37] V. Calsavara, E. Falabella Sousa-Aguiar, N. R. C. Fernandes Machado, *Zeolites* **1996**, *17*, 340–345.
[38] D. L. Liu, S. L. Bao, Q. H. Xu, *Zeolites* **1997**, *18*, 162–170.
[39] T. Sano, Y. Nakajima, Z. B. Wang, Y. Kawakami, K. Soga, A. Iwasaki, *Microporous Mater.* **1997**, *12*, 71–77.
[40] C. F. Baes, R. E. Mesmer, *The Hydrolysis of Cations*, Wiley, New York, **1976**, p. 121.
[41] J. F. Le Page, J. Cosyns, P. Courty, *Applied Heterogeneous Catalysis: Design, Manufacture, Use of Solid Catalysts*, Technip, Paris, **1987**, p. 84.
[42] G. Lietz, K. H. Schnabel, Ch. Peuker, Th. Gross, W. Storek, J. Völter, *J. Catal.* **1994**, *148*, 562–568.
[43] W. Lutz, A. Grossmann, M. Bülow, Th. Gross, *Cryst. Res. Technol.* **1990**, *25*, 135–138.
[44] W. Resechetilowski, R. Schöllner, D. Freude, J. Klinowski, *Appl. Catal.* **1989**, *56*, L15–L20.
[45] P. Sarv, C. Fernandez, J. Amoureux, K. Keskinen, *J. Phys. Chem.* **1996**, *100*, 19223–19226.
[46] O. Bortnovsky, Z. Sobalík, B. Wichterlová, Z. Bastl, *J. Catal.* **2002**, *210*, 171–182.
[47] M. Müller, G. Harvey, R. Prins, *Microporous Mesoporous Mater.* **2000**, *34*, 135–147.
[48] J. S. Buchanan, D. H. Olson, S. E. Schramm, *Appl. Catal. A* **2001**, *220*, 223–234.

Received: January 14, 2005
Published online: June 21, 2005